Supporting Information for

Magmatic activity at the slowest spreading rates: insights from a high-resolution earthquake catalog obtained from Gakkel Ridge Deep (Arctic Ocean)

D. Essing[1,2,*], A. Hellbrück[1,3], and V. Schlindwein[1,3]

[1]Alfred-Wegener-Institute, Helmholtz Centre for Polar and Marine Research, Bremerhaven, Germany
[2]Institute for Geology Mineralogy and Geophysics, Ruhr University Bochum, Germany
[3]Faculty of Geosciences, University of Bremen, Germany
[*]Corresponding author: david.essing@rub.de

Author ORCIDs

D. Essing: 0000-0001-7326-7441
A. Hellbrück: 0009-0000-4492-8685
V. Schlindwein: 0000-0001-5570-2753

Contents of this file

Equation S1

Tables S1 and S2

Figures S1 to S5

Captions for Data sets S1 and S2

Additional Supporting Information (Files uploaded separately)

Data sets S1 and S2

Introduction

This supporting information provides one equation, two tables and 5 figures, which are referenced in the main text. It additionally contains captions for the data sets S1 and S2.

Equation S1:

In the presented approach, we downweigh components of templates with a logistic function f that is based on their signal-to-noise (SNR) ratio:

$$f(SNR) = \frac{L}{1+e^{-k(SNR-x_0)}},$$

where

$$L = \frac{1}{number\ stations * number\ components},$$

k = 1.5

$x_0 = 2$ (Duverger et al., 2018).

The logistic function considers the SNR of each component. If the SNR is smaller than 3, the logistic function reduces the influence of the component, ensuring a smaller contribution during template matching.

Table S1:

Station correction terms applied to each station and phase type prior to earthquake location. Application of station correction terms results in more events falling below an RMS threshold of 0.1 s.

Station (depth)	P station correction [s]	S station correction [s]
GKD01 (4089 m)	-0.059	0.120
GKD02 (3927 m)	-0.064	-0.032
GKD03 (3633 m)	0.078	-0.115
GKD03 (3728 m)	0.043	0.027

Table S2:

Summarized information on the template matching approach.

Used frequency band	5-49 Hz
Root-mean-square error cutoff for manually picked events that serve as template	< 0.1 s
vp/vs ratio to predict phase arrivals if manual picks are missing	1.7
Signal-to-Noise ratio (SNR) needed to serve as potential template	>3
Channels needed with SNR>3 to serve as template	>6
Template window length centered around phase arrival	2 s
Median-absolute-deviation of the stacked (overall components, weighted) correlation coefficients to define a new detection	>11

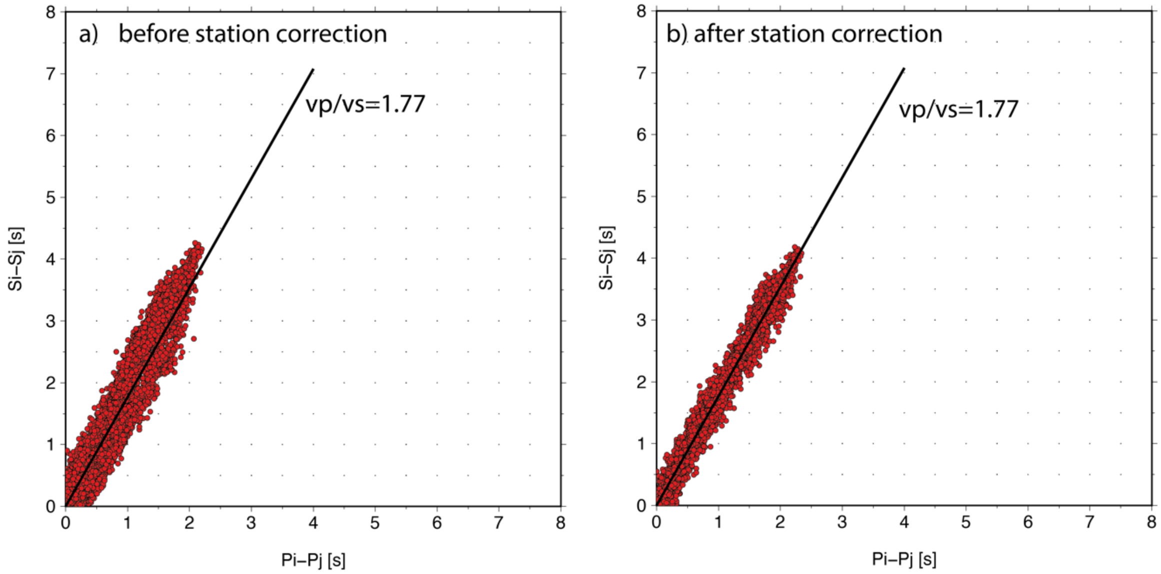

Figure S1. Interstation S-phase time differences for station pairs i,j plotted against interstation P-phase time differences. The figure is based on 1,594 events from the initial 4,503 events that have an RMS<0.1s and 8 phase readings. The data are included in Essing et al. 2024 (data set S2). Note the broad scatter of phase differences around the line with slope 1.77 as estimate for the vp/vs ratio before station correction (a). After station correction (b), scatter is reduced.

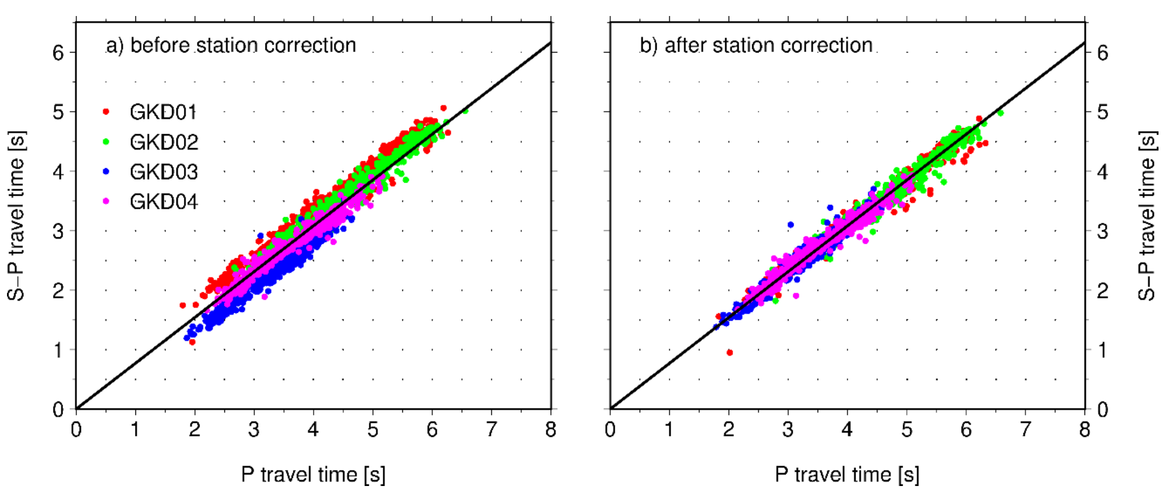

Figure S2. Pseudo-Wadati diagrams illustrating the effect of the station correction for each station. Black line represents a slope of 0.77 and corresponds to a vp/vs ratio of 1.77.

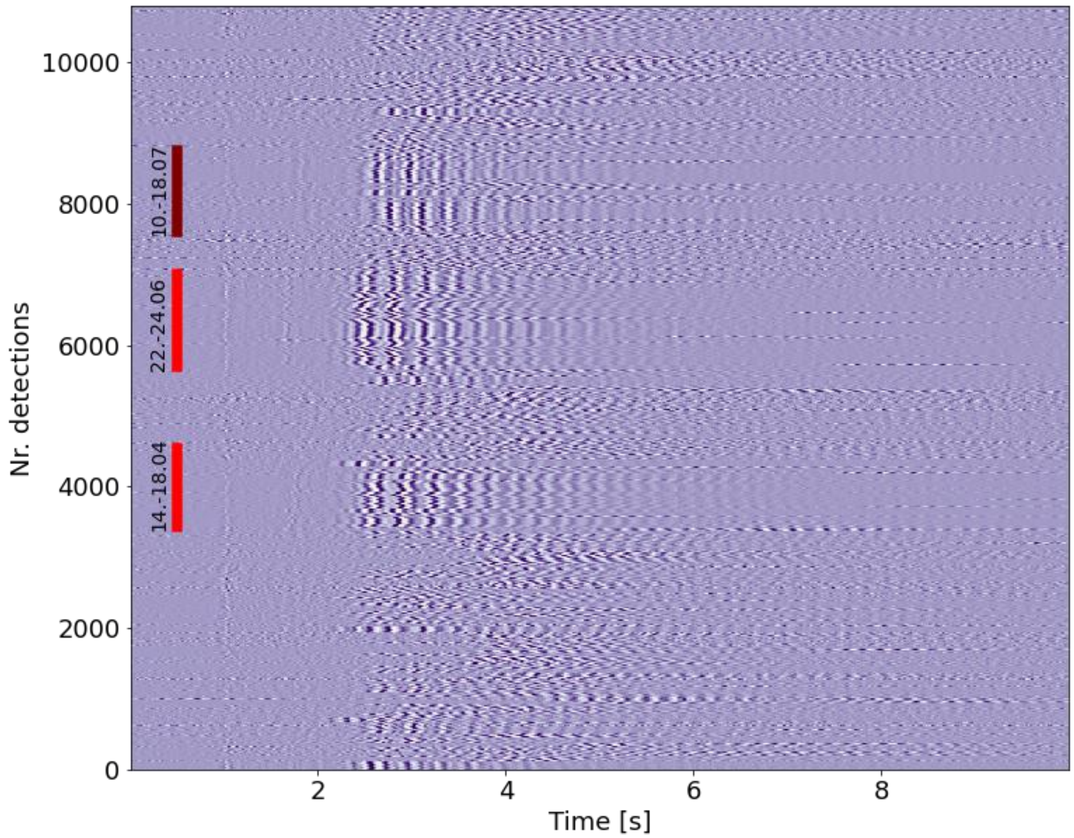

Figure S3. Waveforms of all 10,801 events, recorded at component GKD03.HHZ. Red lines indicate time periods of bursts of seismicity. Note the high similarity of the waveforms in the bursts.

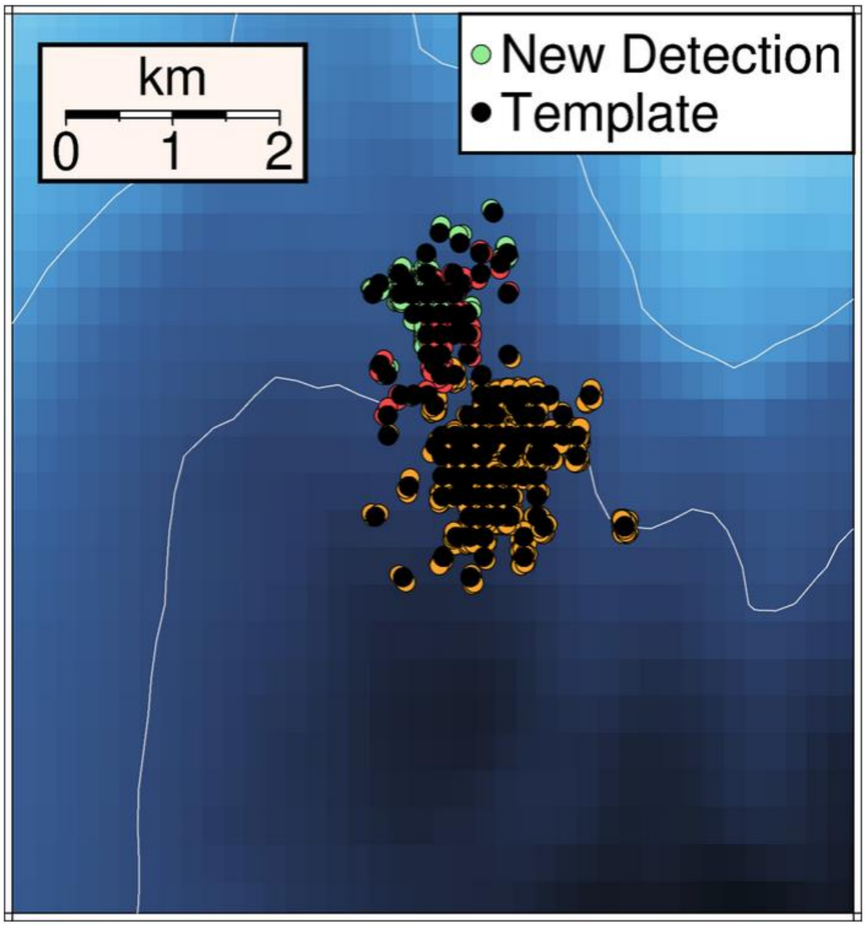

Figure S4. To better visualize the TM-detected events, we add spatial noise to the epicenter location of their detecting template by randomly choosing a value in the range of -0.0025° to +0.0025° longitude and -0.00075° to + 0.00075° latitude. This is done to simulate the collocation of these events to their template event (Essing & Poli, 2022). The locations of new detections and templates are used in Figure 1c.

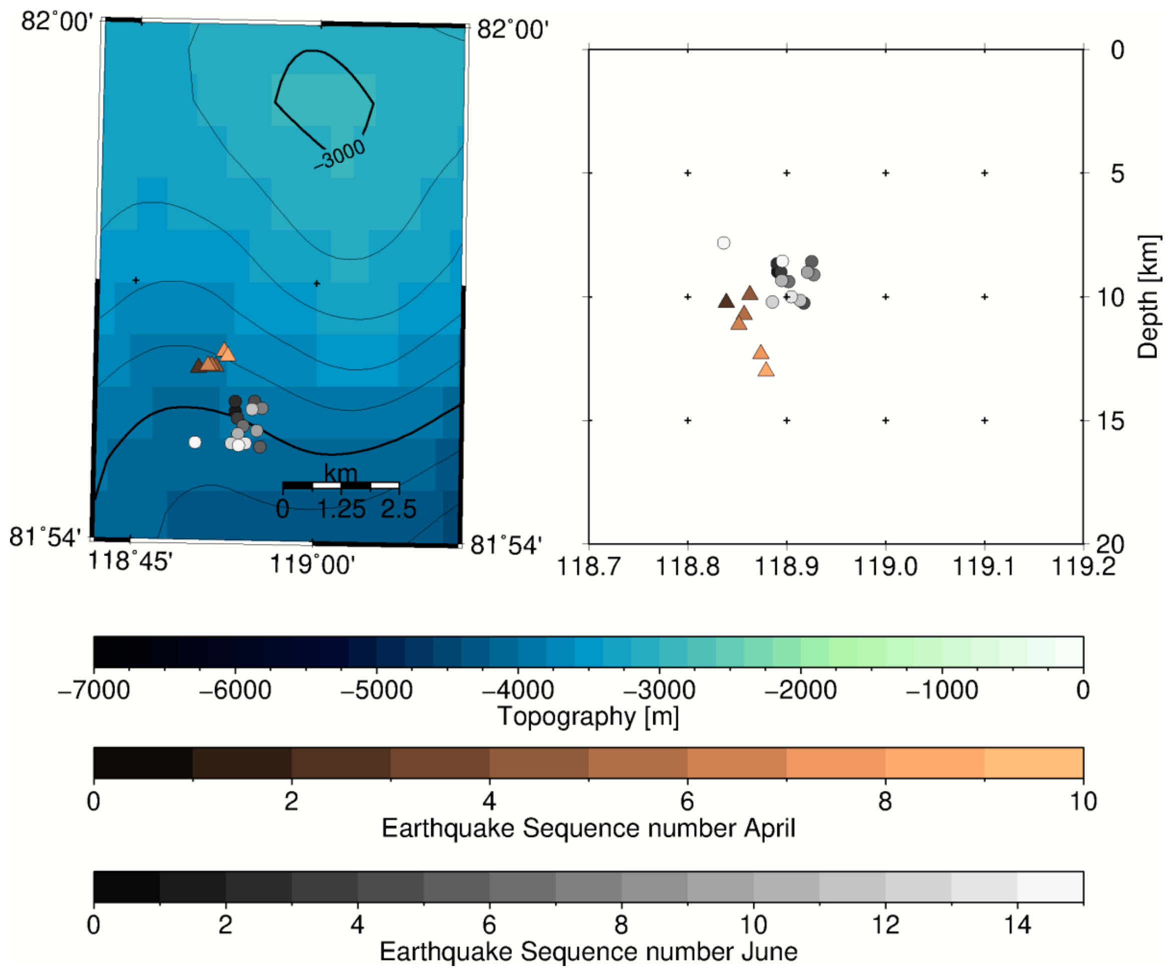

Figure S5. Close-up of the area of seismicity bursts showing the first (brown triangles) and the third (gray circles) of the seismicity bursts in April and June, respectively, in map view (left) and as depth versus longitude plot (right). For both bursts, templates with 7 or more phases readings at the onset of the burst were selected. The clearly observable change in S-P travel time (see Figure 5) is also expressed in changing locations despite location uncertainties larger than the observed migration trend. The April burst exhibits increasing hypocenters depths with time, while the onset of the June burst shows a southward shift of epicenters.

Data Set S1 (Essing, Schlindwein & Hellbrück, 2024)

This data set comprises the catalog of a total of 10801 events, that are either manually picked (CC=1) or new detections. For each detected event we report the origin time (ot), the expectation hypocenter (late, lone, ze), the root-mean-square traveltime residual of the location (rms_template), the estimated magnitude (ml), the ot of the template detecting a given event. The quality of each new detected event is indicated by its ratio between the correlation coefficient and the daily median absolute deviation (MAD) cc_mad_ratio and by the correlation coefficient between the detection and the template cc. As new detections are not relocated, we are using the location of the detecting template.

Data Set S2 (Essing, Schlindwein & Hellbrück, 2024)

Manual picks of 4106 earthquakes that have at least 4 phase readings and are closer than 40 km epicentral distance to one of the four recording stations. An RMS criterion was not applied to the initial 4503 events, but a minimum of 4 phase readings was required and a maximum distance to the recording network of 40 km to impose a minimum quality constraint.

We report the origin date and time of the earthquake, the latitude, longitude and depth of the expectation hypocenter, the error ellipsoid of the location defined as the length of the semi-major axis (Smaj) in km, the length of the semi-minor axis (Smaj) in km, and the azimuth of the semi-major axis relative to geographic north. Deptherr refers to the depth error of the location in km, npha the number of phases used to constrain the location, rms the root-mean-square traveltime residual in s and Ml the local magnitude. The subsequent phase blocks contain the station name (Stat), the recording seismometer component

(Comp), the phase type, the date and time of the phase arrival. Amplitude readings are marked with phase name IAML and additionally contain the amplitude reading in nm and the period in s used to calculate local magnitudes.

References

Duverger, C., Lambotte, S., Bernard, P., Lyon-Caen, H., Deschamps, A., & Nercessian, A. (2018). Dynamics of microseismicity and its relationship with the active structures in the western Corinth Rift (Greece). *Geophysical Journal International, 215*(1), 196-221. DOI:10.1093/gji/ggy264

Essing, D., & Poli, P. (2022). Spatiotemporal Evolution of the Seismicity in the Alto Tiberina Fault System Revealed by a High-Resolution Template Matching Catalog. *Journal of Geophysical Research: Solid Earth*, *127*(10), e2022JB024845. DOI:10.1029/2022JB024845

Essing, D., Schlindwein, V., & Hellbrück, A. (2024). *Earthquake Catalog and Phase-Picks from Gakkel Ridge Deep* [Dataset], Zenodo. DOI:10.5281/zenodo.11261315